Adaptive Switch Matrix for PV Module Connections to Avoid Permanent Cross-Tied Link in PV Array System Under Non-Uniform Irradiations

RUPENDRA KUMAR PACHAURI[1], HASSAN HAES ALHELOU[2,4], (Senior Member, IEEE), JIANBO BAI[3], AND MOHAMAD ESMAIL HAMEDANI GOLSHAN[4], (Senior Member, IEEE)

[1]Department of Electrical and Electronics Engineering, School of Engineering, University of Petroleum and Energy Studies, Dehradun 248007, India
[2]Department of Electrical Power Engineering, Tishreen University, Latakia, Syria
[3]College of Mechanical and Electrical Engineering, Hohai University, Changzhou 213022, China
[4]Department of Electrical and Computer Engineering, Isfahan University of Technology, Isfahan 84156-83111, Iran

Corresponding author: Hassan Haes Alhelou (alhelou@ieee.org)

ABSTRACT In this paper, the significance of cross-tied link between the solar photovoltaic (PV) modules in an array during partial shading conditions (PSCs) is introduced. In order to conduct a detailed analysis, twenty numbers of 20W PV modules (4 × 5) are arranged in a series-parallel (SP) configuration. The change in the pre-arranged SP configured PV array is implemented using a cross-link matrix switch between parallels based on shadow patterns. The switch matrix based modified PV array configuration is called Adaptive-cross-tied (A-CT) configuration. An embedded system based adaptive switch matrix (ASM) controller is developed to control the cross-linking connections between the PV modules under the PSCs to improve global maximum power. In addition, a performance analysis is carried out and compared all PV modules arranged in conventional SP and A-CT configurations. Moreover, realistic shadow test cases are under consideration to characterize current-voltage (I-V) and power-voltage (P-V) characteristics. The output power of the PV array decreases as well as the P-V curves show multiple power maxima points., such as the local maximum power point (LMPP) and the global maximum power point (GMPP). LMPP and GMPP locations, mismatch loss (ML), enhanced fill factor (FF), decreased power loss (PL) and performance ratio (PR) are indicators of performance during experimental and MATLAB/Simulink studies.

INDEX TERMS PV system, power loss, fill factor, current sensor, partial shading conditions, switch matrix controller.

I. INTRODUCTION

In this technological era, electricity plays a key role in the growth of the nation's economy. Most energy demand still relies on fossil fuels, which face major problems with scarcity, limited storage, pollution and high costs for extract and supply, etc. Due to the ongoing shortage of fossil fuels, the popularity of renewable energy (RE) sources have risen over the last few decades. In the context of the urgent need to explore more alternative energy sources and it is found that RE sources are the best choice. Today, PV technology is

The associate editor coordinating the review of this manuscript and approving it for publication was Qiuye Sun.

gaining high attention due to such advantages features as the wide availability of solar energy, simple installation methods and environmentally friendly [1], [2]. Users do not need as much high skills to install and use the PV systems in distinguish low power capacities (10W- 500W), and low maintenance costs. In this sense, the PV industries have continuously growing at a rapid pace in manufacturing and installation fields. In 2018, PV systems can carry the worldwide supply of electricity and a hundred of GW power capacity were added. Thus, the total power capacity of the deployed PV systems worldwide exceeds 505 GW [3].

As far as environmental challenges are concerned and their effects on solar PV efficiency are involved. Moreover, these

climatically issues can be ignored only for short time period. However, on the higher level of the PV power plant side, these environmental problems are resolved with a significant solution. For example, mismatch power losses are a major issue due to hot spot conditions caused by PSCs to limit the PV power output. Moreover, due to the influence of the PSCs, the non-linear behavior of the I-V and P-V curves is observed. The main reasons for this shading are nearby high-rise commercial buildings, telecommunications towers and passing clouds, etc., particularly in urban areas.

Researchers are highly disincentive of the impact of shadowing on PV output. Different methodologies are required to solve these shading issues to enhance System performance. In addition, changing the electrical connections of the PV module in array is one of the strongest approach to enhance the power output under PSCs [4]. In addition, series, SP, total-cross-tied (TCT), bridge link (BL), honey-comb (HC) and many more game /mathematical puzzles based configurations e.g. Su-Do-Ku, Magic square, Latin square and Lo-Shu square etc. are required for extracting maximum power from PV array systems [5]. However, adopted methods to reconfigure PV modules are required high wire length, which is also cause of line losses.

II. LITERATURE REVEIW
The paper consists of a literature study of the most relevant research work, which are reviewed in order to retrieve substantial research gaps [6]–[31]. The different types of PV array configurations are examined in terms of performance, reliability and implementation scope.

In [6], the systematic analysis is carried out and examines the effect of shading with MATLAB/Simulation and experimental testing on I-V and P-V characteristics for series and SP configurations. The performance is further measured in terms of losses (power and current), and improvement in FF, etc. In [7], analyzed the impact of PSCs on various conventional PV array configurations e.g. SP, TCT, HC, BL. In addition, results were calculated with respect to minimal PL and improved FF. In [8], a SP configured PV array is tested experimentally to explore the shadow effect under outdoor and laboratory environment. Obscured sun irradiance level is considered during the investigation, and found parallel connections of PV system have better efficiency. The authors of [9]–[11] developed an ASM for PV array reconfiguration to reduce the shadow effect on PV modules. The research discussed is focused on experimental study of PV array Series, SP, and TCT interconnections. In [12], the authors have compared the outcomes obtained from SP, TCT, and BL configured PV array under climatic conditions. In addition, TCT has the best performance in terms of improved FF and minimized power losses. In [13], a mathematical analysis is undertaken to predict the I-V characteristic behavior under PSCs. For the experimental testing, the findings are matched to show efficient performance. For the analysis of the shading effect, the PV array sizes 6×4 such as SP, and TCT are used. Furthermore, the results obtained from the TCT

set-up indicate dominance over the SP set-up in [14]. For performance assessment, an investigation on I-V and P-V curves is studied [15]–[18]. Moreover, an experimental setup is developed to verify the findings obtained from mathematical analysis. The efficiency of the PV system is also evaluated as per variations in temperature and irradiations. In [19], PV module results based on MATLAB simulations are verified for the P-V characteristics under PSCs by outside experimental results. The PV array is reconfigured and the control of the array optimized by dynamic switch matrix dependent electric connections. A detailed analysis is performed under shaded conditions [20]. The authors of [21] investigated swam optimization approaches based PV array re-configurations to reduce the required wire length as used in puzzle based reconfiguration. Performance matrices are computed for conventional 9×9 size TCT, competence square to show the effective response during PSCs. Flow regime algorithm (FRA) has best performance with the GMPP value 2731W under 400W/m^2, 600W/m^2 and 900W/m^2 compare to Genetic algorithm, social mimic optimization algorithm (SMO), and the Rao optimization algorithms. GMPP location is identified as 4.297kW, 5.04212kW; 3.712kW and 4.863kW under four distinguish non-uniform irradiation levels from 200-900W/m^2. The grasshopper optimization algorithm (GOA) is proposed to enhance the PV array performance compared to TCT, Su-Do-Ku and GA based configurations. With respect to TCT configuration, power enhancement is observed as 3.361%, 10.949%, 0.8647% and 6.7481% under all four shading scenarios [22]. Using Latin Square puzzle, TCT arrangement is reconfigured and entitled LS-TCT configuration. Investigated under four progressive shading conditions. LS-TCT has best performance in term of GMPP (2279W, 2139W, 1806W, 1680W), FF (9.91, 9.26, 7.85, 7.30) and reduced power losses (330W, 470W, 803W, 929W) respectively [23]. In [24, 25], conventional Su-Do-Ku pattern is improved to enhance shade dispersion property under shading conditions from 100-700W/m^2 and 1000W/m^2. Improve So-Do-Ku configuration has best performance in terms of efficiency, FF and mismatch losses 11.79%, 65.8% and 11.25% compared with SP, BL, HC, TCT, Su-Do-Ku and Optimal Su-Do-Ku configurations under shading case-III. In [26], proposed reconfigure method (RM) arrangement is carried out to reconfigure PV array and compared with existing SP, BL and TCT configurations under non-uniform irradiations 400W/m^2, 500W/m^2, 700W/m^2 and 1000W/m^2. Highest peak power is achieved in case of RM configuration as 3.71kW compared to SP, BL and TCT (3.6kW, 3.42kW and 3.6kW) respectively under shading fault case-II. In [27], modified Harris hawks optimizer (HHO) is helpful to enhance the shade dispersion as compared TCT, CS, HHO based configurations. GMPP location of MHHO configuration is observed as 2475.99W. Minimized PL 31.76%, 41.114%, 18.701% and 21.729% during all four PSCs (200W/m^2, 400W/m^2, 600W/m^2, 800W/m^2 and 900W/m^2). In [28], an efficient approach based on artificial ecosystem-based optimization (AEO) is used to reduce

PL. In addition, the proposed AEO method is compared with TCT, HHO and conventional PSO methods to show higher GMPP values at 89504W, 84927W, 88554W and 88554W respectively under 200W/m², 450W/m², 600W/m² and 900W/m². Gray wolf optimizing technique is correlated with TCT, Su-Do-Ku configurations in terms of GMPPs such as 1308.39W, 12074.41W and 12982.28W respectively under non-uniform irradiation as 400W/m², 600W/m² and 1000W/m² [29], [30]. Comprehensive study is performed on conventional SP, BL, HC and TCT PV array configurations, and compared to the three possible integer number combinations of Su-Do-Ku configurations under PSCs. Improved Su-Do-Ku configuration has higher side GMPP and different performance aspects are analyzed effectively [31].

PV power plants have been widely used in power industry with advanced technological aspects such as battery system integration, energy internet and sensor network systems [32]–[34]. However, the performance of PV power plants still has the potential to improve. The proposed reconfiguration scheme for PV modules is particularly advantageous for the design of large PV plants.

A. NOVELTY OF WORK

It is observed that from last five years, the authors have focused on the reconfiguration methods to enhance the PV system performance. However, the authors have neglected the disadvantage of this reconfiguration process, such as the high wire length needed and the permanent risk of line losses. In this context, an idea is raised to avoid mathematical puzzle based reconfiguration of PV array system. An ASM is considered to reform the PV module connections in an array system to avoid the effect of PSCs. During experimental and MATLAB/Simulink study, following salient points are claimed as a novelty of work,

- The modifications in 4×5 size SP configured PV array are carried using embedded system based ASM.
- Proposed A-CT configuration is compared with the conventional SP, BL, HC configurations under distinguish PSCs in terms of hardware and performance reliability.
- LMPP and GMPP locations, ML, improved FF, reduced PL and PR are shown as remarkable performance indices comprehensively.
- Proposed A-CT configuration has best results under climatically shading scenarios with respect to conventional configurations and require less wire length to reconfigure using ASM approach.

This paper is arranged in a total of six sections. Section II concerns the literature review and the novelty of the work. In addition, the experimental setup and specifications of the supporting components are defined in section III. The PV array modelling, performance assessment and shadowing pattern analysis are discussed in Section IV. Section V contains the conclusions and discussion of this article. Section VI is accompanied by a conclusion at the end of the manuscript.

III. EXPERIMENTAL SETUP AND SPECIFICATIONS

The developed hardware model consisted mainly of three sections such as (i) 4×5 size PV array (ii) Electrical parameters measurement unit (iii) SMC unit (iv) Data acquisition system (DAS). The experimental setup, schematic diagram and flow chart to represent the system operation are given in Fig. 1-3 respectively. In addition, the specifications and supporting role of all the components used during the experimental study are reported in Table 1 as,

IV. SOLAR PV TECHNOLOGY

A. PV SYSTEM MODELLING

Here the PV equivalent model is based on the single diode model [35]. PV cell is considered to be a variable current source parallel to photodiode – current (I_{ph}) and can be expressed as,

$$I_{ph} = (I_{SC} + K_i \Delta T) \left(\frac{S}{S_{STC}} \right) \frac{(R_{sh} + R_{se})}{R_{sh}} \quad (1)$$

where, R_{se} and R_{sh} are PV cell series and shunt resistance respectively, short circuit (S. C.) current and solar irradiance are expressed as I_{SC} and S_x, K_i – Cell temperature coefficient [35]. PV surface temperature is determined with help of actual temperature (T_x) and standard test condition temperature (T_{ST}) as,

$$\Delta T = (T - T_{ST}) \quad (2)$$

Similar PV cells and bypass diodes are inter linked in the PV module to avoid damage from hot spot phenomenon under PSCs. An electrical equivalent model of PV module is depicted in Fig. 4 [35]. The module current expression with bypass diode is shown in Eq. (3) as,

$$I_{mod} = \left\{ I_{ph} - I_o \left(e^{\frac{q(V_{mod} + R_s I_{pv})}{AKTN_s}} - 1 \right) - \frac{V_{mod} + R_s I_{pv}}{R_{sh} N_s} \right\} + \left\{ I_{obypass} \left(e^{\frac{-q(V_{mod})}{A_{bypass}}} - 1 \right) \right\} \quad (3)$$

where, A and I_o are ideality factor and reverse saturation current respectively. K – Boltzmann constant (1.38×10^{-23} J/K), T states Kelvin temperature, and q is electron charge (1.6×10^{-19}° C), V_{module} – module output voltage. N_s – Cascaded connection of solar cells to design a PV module, R_{S-mod} and R_{sh-mod} are series and shunt module resistances respectively.

B. PV SYSTEM MODELLING

Researchers are thoroughly studying the design of the PV module arrays. The design methodologies for all the PV array configurations are given with the aspect of structure and voltage and current analysis.

1) SERIES-PARALLEL

PV modules are arranged in series connections to form a string, followed by parallel modules, as shown in Fig. 5(a). These multiple strings are referred to as the SP circuit, which increases the current for load output matching.

TABLE 1. Role of supporting components used in the experimental setup evolved.

Section	Components	Specifications	Role/function
1. Solar PV system	PV modules in array (4×5 size)	• PV module max. power: 20W • I_{sc}: 1.19A, V_{oc}: 22.58V • I_m: 1.08A, V_m: 18.82V • No. of PV module: 4 (2×2) • Cell technology: Poly-Si • Dimension (mm): 356×490×25 • Manf.: Spark Solar Pvt. Ltd. • Model: SS2018P	20 numbers of PV modules are arranged with a switch matrix to be reconfigured.
2. Electrical parameters measurement unit	Voltage sensor (Arduino compatible)	• Number of voltage sensor: 1 • Input voltage: 0 to 120V DC (Modified). • Voltage detection range: 0.02445 -120 V. • Analog voltage resolution: 0.00489	• Sensor module enables the measurement of 0-120V. • The actual voltage of the PV module is obtained after calibration.
	Current sensor (Arduino compatible)	• No. of current sensor: 1 • Measurement range: 0.01 to 20A DC • Scale Factor: 100 mV per Amp • Model: ACS712ELC	• Sensor module is based on hall effect operation.
	Arduino –Nano	• Microcontroller: ATmega328 • Required supply voltage: +5V • Digital I/O pins: 14 • Analog I/P pins: 8 • Flash memory: 16 KB • Temperature Range:-40°C to 85°C	• Open source Arduino-nano (16 MHz frequency oscillator) system utilized in data logger system.
	Liquid crystal display	• Size: 16×2 • Supply voltage: +5V • Data pins: 8- bit	• To display real time voltage and current values during the investigation.
	Personal Computer system	• Windows PC system with Arduino open source.	• Needed to write and upload code to the setup of Arduino-UNO. • Use to real time data recording.
3. Switch matrix control unit	Electro-mechanical relay	• +5V DC operated	• Used as switches to reconfigure PV array
	Arduino- mega	• Input output terminals: 54 • Analog inputs: 16 • Operating voltage: 6-12 V DC	• Open source Arduino-Mega (16 MHz frequency oscillator) system utilized to control relay operation in switch matrix.
4. Load and solar irradiation measurement	Variable decade resistive load	• Range: 0- 360 Ω, 5 A	• Used to characterize the solar PV array from 0 Ω to maximum value of resistive load.
	Pyrometer	• Sun Irradiation measurement up to 1999 W/m² • Resolution: 1 W/m²	• During experimentation to measure solar irradiation in W/m².

2) BRIDGE-LINK

The bridge architecture is being used for connecting PV modules as shown in Fig. 5(b). If configurations of this kind are partially shaded, the adjacent modules will also be affected, increasing the total voltage and current output.

3) HONEY-COMB

In the honeycomb configuration, PV modules are visualized in Fig. 5(c). In some, but not all, shading conditions, these configurations can cause common power output losses. Consequently, HC architecture vulnerability lacks robustness.

4) ADAPTIVE CROSS-TIED

All parallel strings are cross-linked and this design includes a mechanism for linking the modules in parallel and in sequence. This mechanism can solve drawbacks in series and parallel arrays. Relay switches are used to transform current SP configurations as shown in Fig. 5(d).

The voltage, current, and power outputs of the four PV module connection schemes are summarized in Table 2. The power outputs of the four configurations mentioned previously are approximately equal at identical irradiation levels when no shading or malfunctions occur. However, when
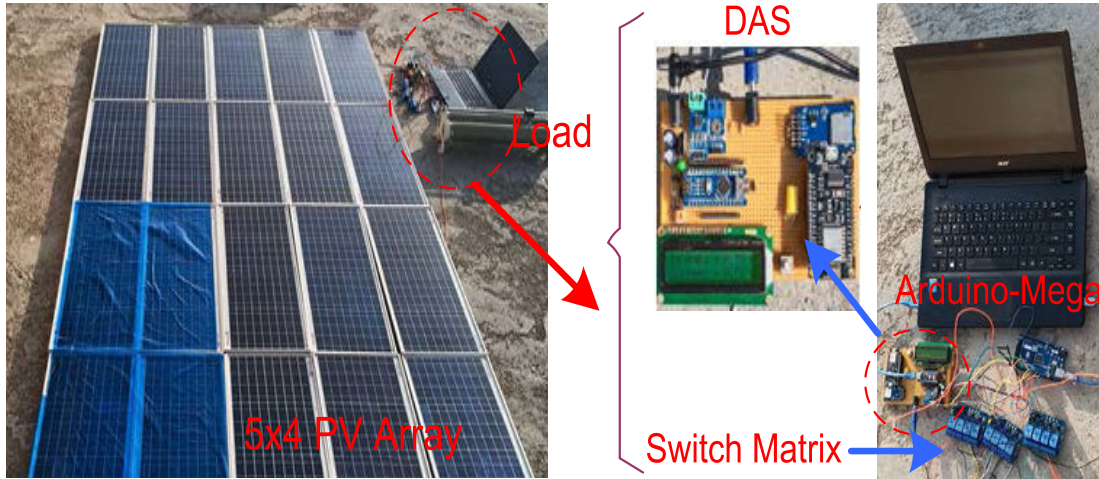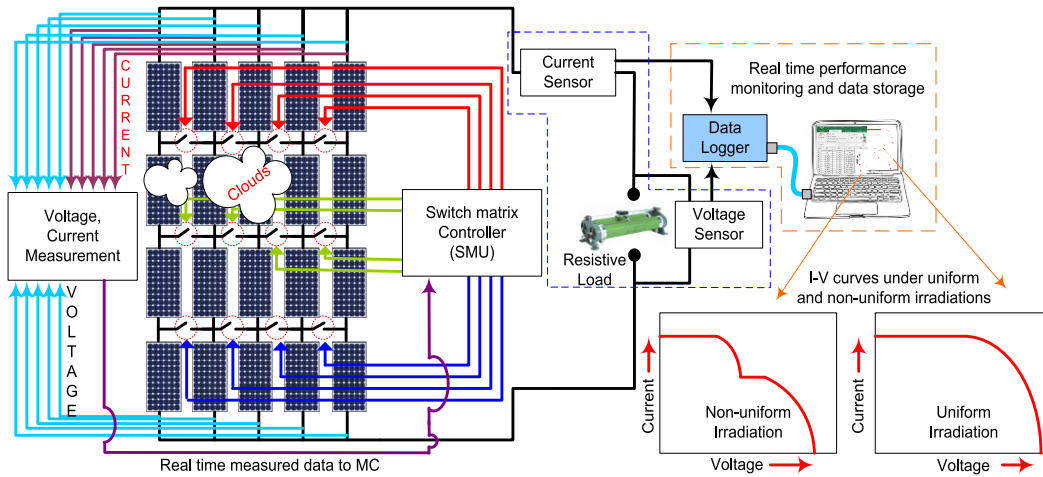
FIGURE 1. Experimental setup.

FIGURE 2. Schematic diagram of system.

shading or malfunctions occur, the power outputs of the configurations differ primarily because of differences in the connection schemes. When a PV module is shaded, its voltage and current outputs are reduced, which further lowers the voltage and current outputs of neighboring series- or parallel-connected PV modules, thereby inducing a decline in the overall power output. Accordingly, this study proposes a strategy for optimizing the configuration of module arrays when shading or malfunctions occur to improve the power output of PV module arrays even in shaded or malfunction conditions. In Table 3, number of functional cross-tied during shading cases for all the PV array configurations are depicted.

C. PERFORMANCE PARAMETERS AND PARTIAL SHADING ANALYSIS

The current produced by 5×4 size PV array system depends on the solar irradiation directly and shown in Eq. (4) as,

$$I = \left(\frac{S}{S_{STC}}\right) I_m \qquad (4)$$

where, I_m is the PV module current at STC ($S_{STC} = 1000 W/m^2$ and $T = 25°C$. S_x stands for actual irradiation.

Applying Kirchhoff's Voltage Law, the assessment of PV array voltage can be done and expressed as Eq. (5) as,

$$V = \sum_{n=1}^{5} V_{mn} \qquad (5)$$

where, V_{mn} is the maximum voltage of nth row of the PV array and PL can be expressed, *PL = Power at MPP during uniform irradiation − Power at GMPP during non-uniform irradiation*

Due to this PL condition under non-uniform irradiation, FF changes are caused, which depend on the PV array's V_{oc} and I_{sc}. With the variation of shading, affected FF is evaluated using Eq. (6) as,

$$FF = \frac{V_{mpp} I_{mpp}}{V_{OC} I_{SC}} \qquad (6)$$

PE is the increment in power produced in the reconfigured scheme of PV array due to shade dispersion and expressed in Eq. (7) as,

$$\%PE = \frac{GMPP_{A-CT} - GMPP_{TCT}}{GMPP_{A-CT}} \times 100 \qquad (7)$$

TABLE 2. Voltage, current and power under ideal conditions.

Configuration	Electrical Performance		
	V_{array}	I_{array}	P_{array}
SP	$V = \sum_{n=1}^{4} V_n = 4V$	$I = \sum_{n=1}^{5} I_n = 5I$	$P = 20VI$
BL	$V = \sum_{n=1}^{4} V_n = 4V$	$I = \sum_{n=1}^{5} I_n = 5I$	$P = 20VI$
HC	$V = \sum_{n=1}^{4} V_n = 4V$	$I = \sum_{n=1}^{5} I_n = 5I$	$P = 20VI$
A-CT	$V = \sum_{n=1}^{4} V_n = 4V$	$I = \sum_{n=1}^{5} I_n = 5I$	$P = 20VI$

*V, I are the output voltage and current respectively

TABLE 3. Number of functional cross-tied during shading cases.

PV array	Total cross-ties	Number of functional cross-ties during shading cases				% Utilization
		Case- I	Case-II	Case-III	Case-IV	
SP	-	-	-	-	-	-
BL	6	6	6	6	6	100
HC	4	4	4	4	4	100
A-CT	12	4	5	4	4	30-35

In high density urban areas, most of the shadow causes are introduced due to high-rise buildings, shopping malls and telecom towers etc. But all the shadowing causes having its predefined shading patterns due to dynamic position of sun irradiance over a day-time period. In Fig. 6, the four realistic shading patterns are acknowledged in this article viz. building corner shading, single row-column shading, street light pole shading and random shading scenario. Moreover, these considered shading patterns are suitable and likely to appear in a 5×4 size of PV array. This research article comprehensively discusses the impact on shading conditions and perceived on performance output of PV system configurations.

V. RESULTS AND DISCUSSION

In present study, the effects of the considered shading cases I-IV on the performance of the SP and A-CT configurations are investigated through experimental and simulation aspects. Under STC, the current generated from integrated all PV modules in an array is assumed I_n. Theoretically, the row currents in PV array systems are expressed under shading cases I- IV are given from Eq. (8)-(17) as,

For shading case-I

$$I_{r_1} = I_{r_2} = 0.445I_n + 0.445I_n + 0.88I_n + 0.88I_n + 0.88I_n$$
$$= 3.557I_n \tag{8}$$
$$I_{r_3} = I_{r_4} = 0.88I_n + 0.88I_n + 0.88I_n + 0.88I_n + 0.88I_n$$
$$= 4.4I_n \tag{9}$$

For shading case-II

$$I_{r_1} = 0.88I_n + 0.445I_n + 0.445I_n + 0.445I_n + 0.445I_n$$

$$= 2.66I_n \tag{10}$$
$$I_{r_2} = I_{r_3} = I_{r_4} = 0.88I_n + 0.88I_n + 0.88I_n + 0.88I_n$$
$$+0.445I_n = 3.965I_n \tag{11}$$

For shading case-III

$$I_{r_1} = 0.88I_n + 0.88I_n + 0.88I_n + 0.88I_n + 0.88I_n$$
$$= 4.4I_n \tag{12}$$
$$I_{r_2} = I_{r_4} = 0.88I_n + 0.88I_n + 0.445I_n + 0.445I_n + 0.88I_n$$
$$= 3.53I_n \tag{13}$$
$$I_{r_3} = 0.445I_n + 0.445I_n + 0.445I_n + 0.445I_n + 0.88I_n$$
$$= 2.66I_n \tag{14}$$

For shading case-IV

$$I_{r_1} = 0.305I_n + 0.88I_n + 0.445I_n + 0.305I_n + 0.305I_n$$
$$= 2.24I_n \tag{15}$$
$$I_{r_2} = I_{r_3} = 0.445I_n + 0.88I_n + 0.88I_n + 0.88I_n + 0.455I_n$$
$$= 3.53I_n \tag{16}$$
$$I_{r_4} = 0.88I_n + 0.88I_n + 0.88I_n + 0.88I_n + 0.88I_n$$
$$= 4.4I_n \tag{17}$$

Ignorance of all the little bit voltage imbalances found across each row and that of the voltage observed across PV array is represented in Eq. (18) as,

$$P_{array} = V_{array} \times 5V_n \tag{18}$$

For the purpose of performance parameter assessment, it is necessary to understand the behavior of P-V and I-V characteristics, shown in Fig. 6 as,
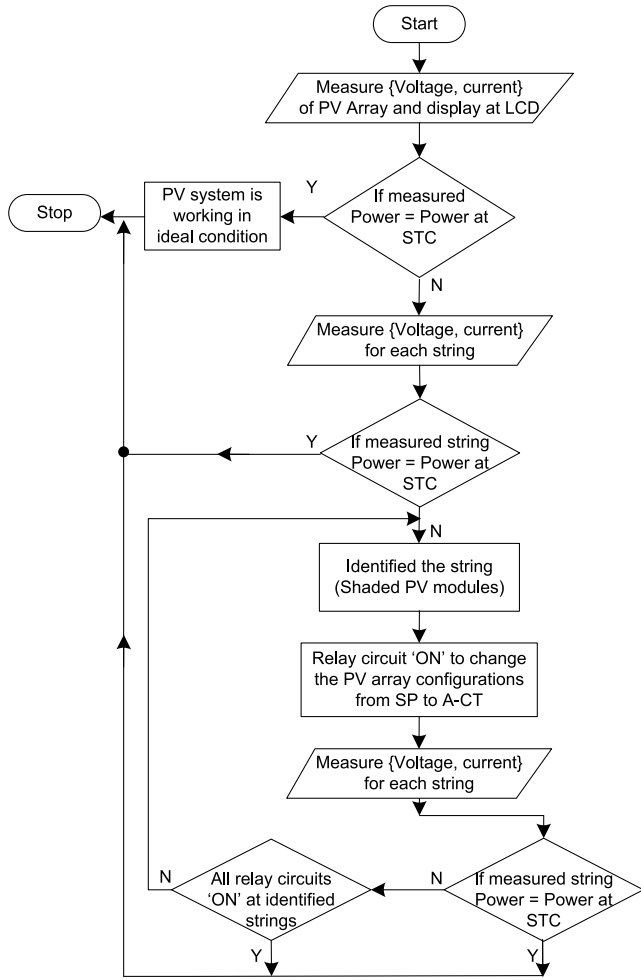
FIGURE 3. Flow chart for system operation.
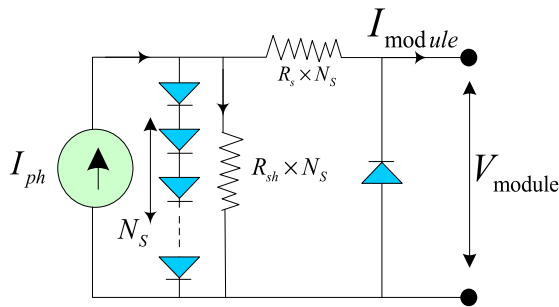
FIGURE 4. Electrical equivalent circuit of a PV cell [35].

The hardware setup is useful for detailed analysis to verify the findings of the MATLAB/Simulink study. Both effects of the PSCs on the PV system are critically studied in order to obtain output parameters due to the smooth action of the P-V and I-V characteristics. Investigation carried out during the PSCs, obviously a high change of existence of numbers of LMPP and GMPP on I-V and P-V performance characteristics. The multi peaks such as LMPP and GMPP create a big disturbance to track actual MPP (higher value) by the maximum power point tracking (MPPT) devices. In present study, switching control methodology for electrical interconnection

FIGURE 5. (a)-(d).PV array configurations.

between PV modules is adopted to minimize the multiple MPP on P-V characteristics.

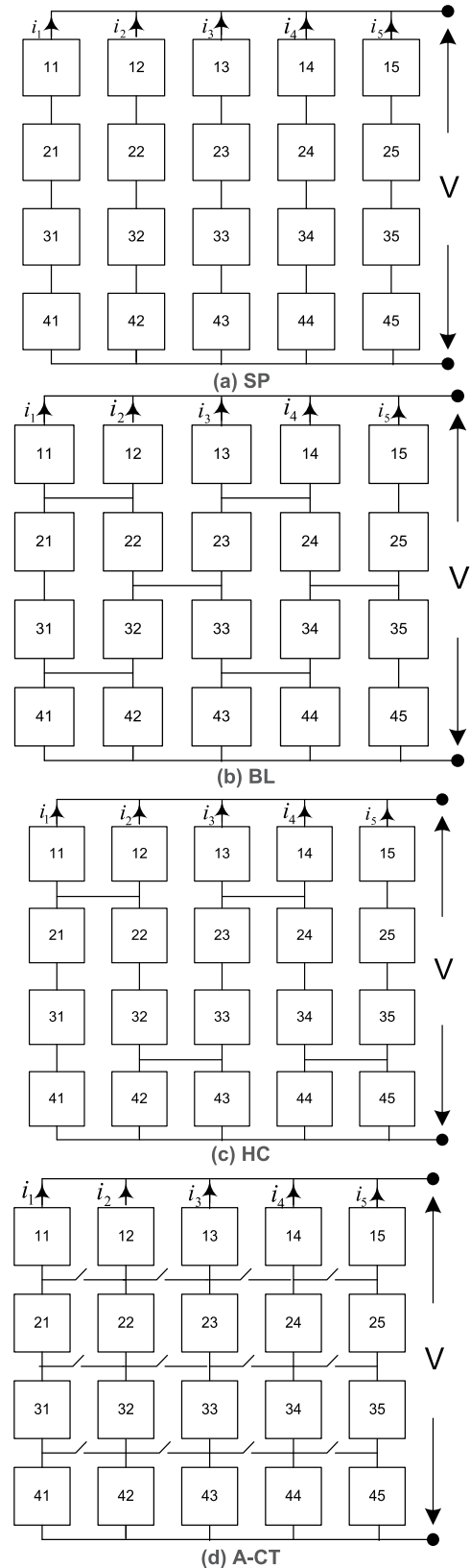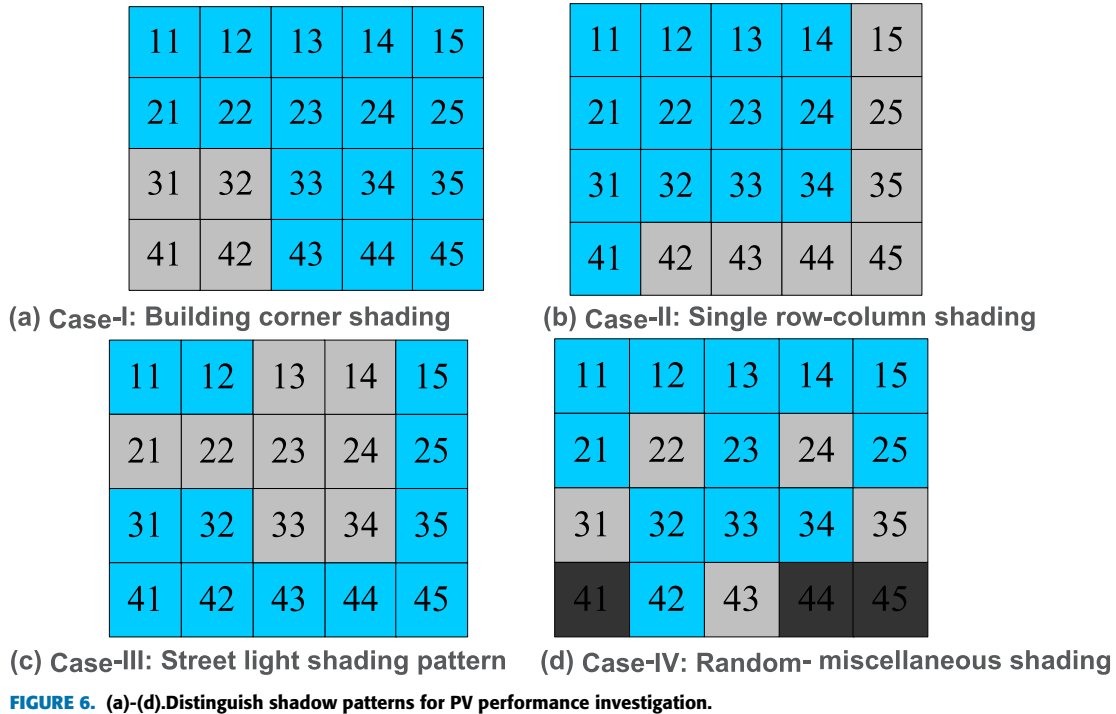| 11	12	13	14	15
21	22	23	24	25
31	32	33	34	35
41	42	43	44	45

(a) Case-I: Building corner shading

11	12	13	14	15
21	22	23	24	25
31	32	33	34	35
41	42	43	44	45

(b) Case-II: Single row-column shading

11	12	13	14	15
21	22	23	24	25
31	32	33	34	35
41	42	43	44	45

(c) Case-III: Street light shading pattern

11	12	13	14	15
21	22	23	24	25
31	32	33	34	35
41	42	43	44	45

(d) Case-IV: Random- miscellaneous shading

FIGURE 6. (a)-(d).Distinguish shadow patterns for PV performance investigation.

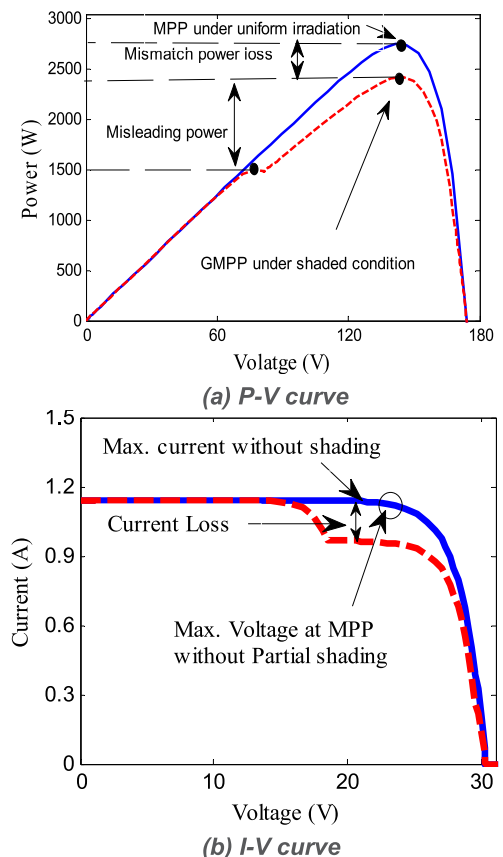## A. P-V AND I-V CHARACTERISTICS OF SOLAR PV ARRAY UNDER SHADING CASE-I

A detailed analysis on the accomplished performance of SP, BL, HC and proposed A-CT configurations is deliberated. For MATLAB/Simulink and experimental analysis under shading cases I-IV, the behaviour of obtained P-V and I-V curves for PV array configurations is studied and shown in figure 7(a)-(b). The SP, BL and HC configurations are experiencing a considerable amount of shading due to the lack of coherence between the module's maxima power and GMPP of PV array compared to proposed A-CT configuration.

In shading case-I, the GMPP of the SP, BL, and HC configurations are observed as 283.4W, 288.7W, 284.1W at two different irradiation levels such as 880W/m^2 and 445W/m^2. For the suggested A-CT configuration, the GMPP is observed on the higher side as 291.3W relative to conventional PV array configurations. The GMPP of the SP, BL, and HC configurations are reported as 281W, 288.2W, and 284W as result of the experimental study to verify the simulation results.

In addition, for A-CT configuration, the GMPP is observed as 288.7W compared to conventional PV array configurations. During MATLAB simulation and experiment, the performance output of considered PV array configurations is contrasted based on the smoothness of the P-V curves under PSCs.

In addition, the non-linear aspect of the I-V characteristics of SP, BL, and HC arrangements for different shading cases of the PV array is observed. The acquired S. C. current of A-TCT configuration is found to be similar to other configurations for simulation and experimental studies under all the

(a) P-V curve

(b) I-V curve

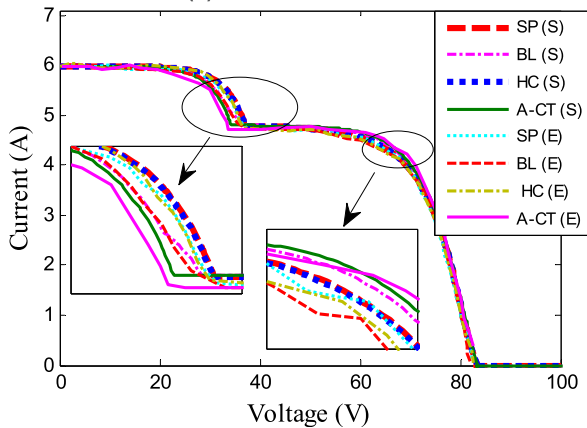**FIGURE 7.** Electrical characteristics of PV system.

PSCs. For all PV array configurations, such as 5.982A for simulation and 5.96A, 5.97A, 5.96A and 5.98A for experimental studies, the values of S. C. current are observed under shading case-I.
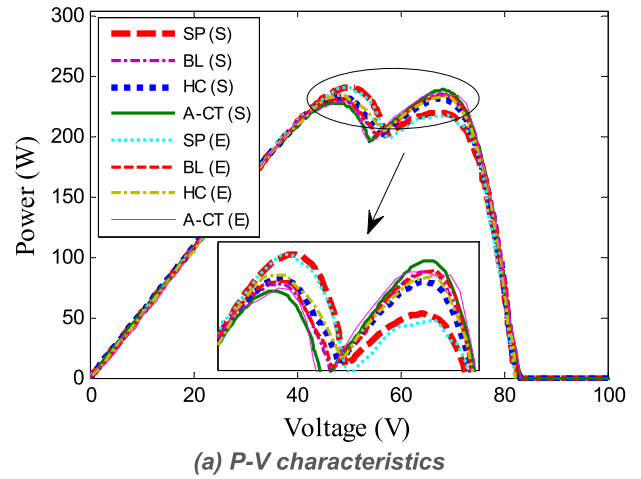
(a) P-V characteristics
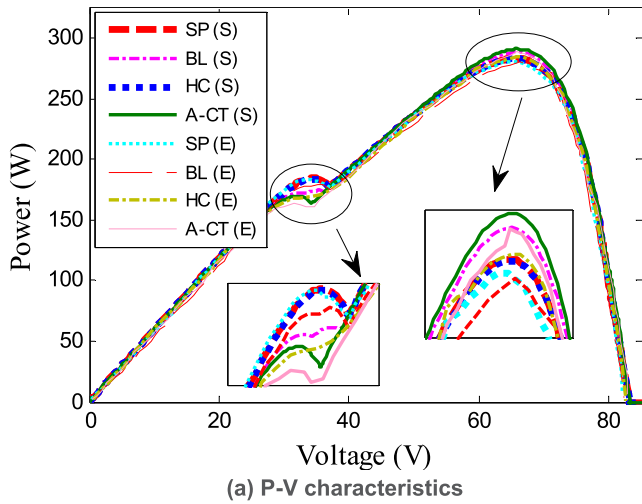
(a) P-V characteristics

(a) I-V characteristics

FIGURE 8. (a)-(b) Performance characteristics under shading case-I.

(b) I-V characteristics

FIGURE 9. (a)-(b) Performance characteristics under shading case-II.

B. P-V AND I-V CHARACTERISTICS OF SOLAR PV ARRAY UNDER SHADING CASE-II
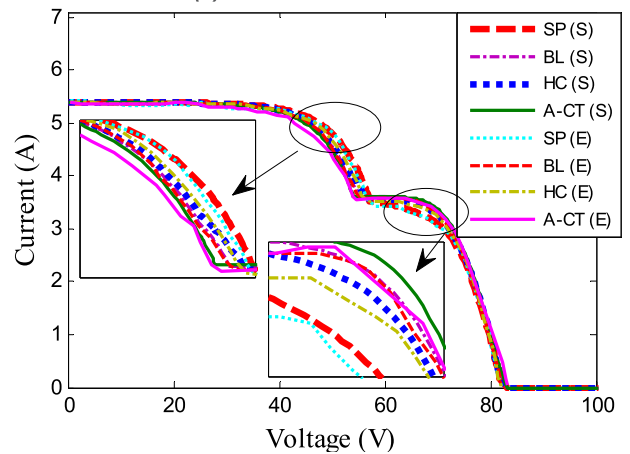
A study on how well the SP, BL, HC, and A-CT configurations worked is deliberated. The behaviour of P-V and I-V curves obtained from PV array configurations is investigated for MATLAB/Simulink and experimental analysis under shading case- II and shown in figure 8(a)- (b). The SP, BL and HC configurations are experienced the PL because of non-coherence phenomenon of GMPP between PV arrays compared to A-CT configuration.

The GMPP position of the SP, BL, and HC configurations is noted as 231.1W, 234.4W, 233W under non-uniform irradiation levels in shading case-II. The GMPP is observed on the higher side as 238.2W in the proposed A-CT configuration. The GMPP position of the SP, BL, and HC configurations is specified as 227.7W, 233.2W, 232.6W under similar irradiation levels as part of the experimental analysis. In addition, the GMPP for the A-CT configuration is noted as 234.3W.

In addition, under PSCs, the I-V features of SP, BL, and HC arrangements are observed. During simulation and experimental studies, the acquired S. C. current of A-TCT was found to be identical to other configurations. S. C. current values for all PV array configurations, such as 5.392A

for simulation and 5.435A, 5.383A, 5.40A and 5.365A for experimental studies, are found to be identical under shading case-II.

C. P-V AND I-V CHARACTERISTICS OF SOLAR PV ARRAY UNDER SHADING CASE-III

Power observation at GMPP is determined by the occurrence of several maximum points on P-V curves. Under the shading case-III, for simulation analysis, power at GMPPs is observed for SP, BL, HC and A-CT configurations as 218.2W, 219.8W, 224.7W and 234.7W respectively. In addition, during experimental analysis, GMPP positions are observed to confirm the effects of shading as 216.5W, 217.9W, 220.9W, and 232W. Among the considered PV array configurations during simulation testing, the A-TCT configuration has the highest power at GMPP.

Under shading case-III, the behaviour of the I-V characteristic of SP, BL, HC and A-CT configurations is investigated. In addition, the obtained S. C. current of the A-TCT is found to be identical to other configurations during simulation and experimental studies. In fact, S. C. current values are identical for all PV array configuration such as 5.982A for simulation and 5.97A, 5.96A, 5.965A and 5.96A for experimental
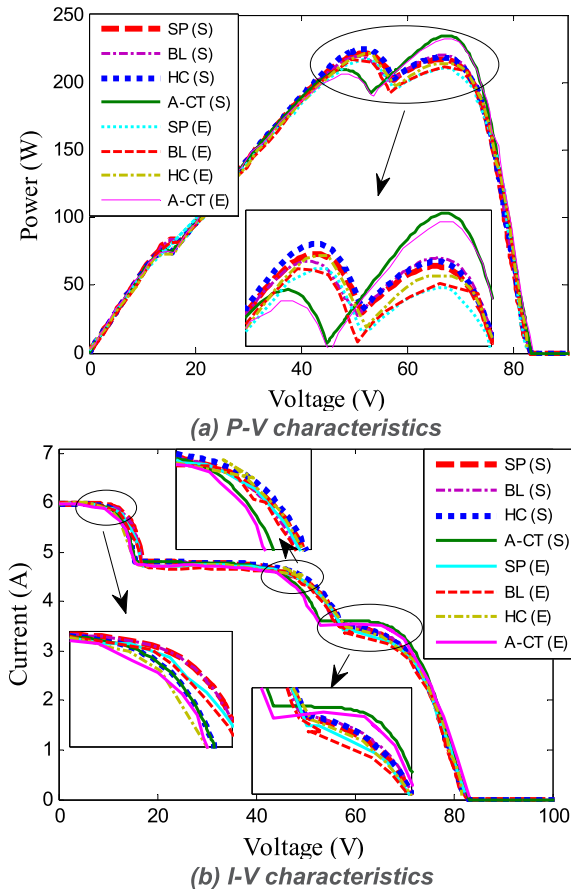
(a) P-V characteristics

(b) I-V characteristics

FIGURE 10. (a)-(b) Performance characteristics under shading case-III.

(a) P-V characteristics

(b) I-V characteristics

FIGURE 11. (a)-(b) Performance characteristics under shading case-IV.

studies respectively. The behaviour of P-V and I-V curves obtained from PV array configurations is investigated for MATLAB/Simulink and experimental study under shading case- III and shown in figure 9(a)-(b).

D. P-V AND I-V CHARACTERISTICS OF SOLAR PV ARRAY UNDER SHADING CASE-IV

The estimation of the GMPP location is carried out via the presence of several P-V maxima points. For SP, BL, HC and A-CT configurations, power at GMPPs is observed as 190.4W, 198.2W, 192.3W and 202.14W respectively for simulation analysis under the shading case-IV. In addition, during experimental tests, GMPP positions are recognized as 189.4W, 197.5W, 192.80W, and 199.5W to check the effects of simulation. Among the considered PV array configurations during simulation analysis, the A-TCT configuration has the highest power at GMPP.

The behaviour of the I-V characteristic of the SP, BL, HC and A-CT configurations is studied in the case-IV shading. In addition, the SC current obtained from A-TCT is found to be identical to other configurations during simulation and experimental studies. In this sense, the existing SC values are 5.98A, 5.96A, 5.98A and 5.98A for all simulation PV array configurations and 5.96A, 5.96A, 5.89A and 5.96A for experimental studies, respectively. The P-V and I-V curves
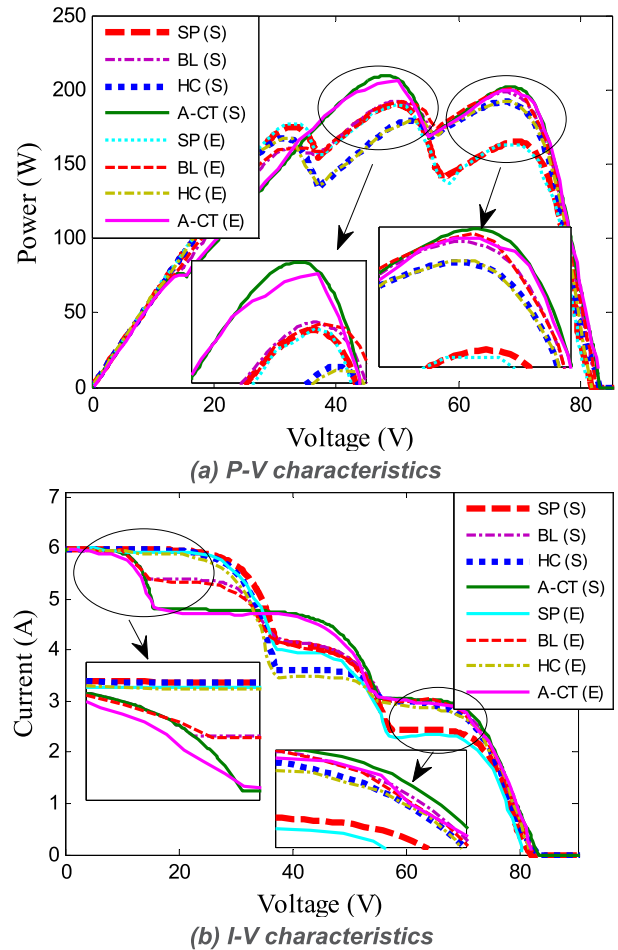
obtained from the PV array configurations are investigated in the MATLAB/Simulink and experimental analysis and shown in Figure 10(a) - (b).

E. POWER AT GMPP

Investigation to identify the GMPP location in between local and global values of power maxima is analyzed. Simulation and experimental results in terms of power at GMPP are shown in figure 11 and Table 4. Highest power at GMPP is obtained as 291.3W, 238.2W 234.7W and 202.14W for A-CT configuration under shading cases I-IV during MAT-LAB/Simulink study. In addition, higher power at GMPP is obtained as 288.7W, 234.3W, 232W and 199.5W for A-CT as related to classical SP, BL, and HC configurations under shading cases I-IV during experimentation.

F. VOLTAGE AT GMPP

Voltage at GMPP is very important parameters for delivering power to the load side. In MATLAB/Simulation study, voltage at GMPP for SP, BL, HC and A-CT Configurations have distinguishing values under shading case-I (65.5V, 65.73W, 65.5V and 65.9V), case-II (50.26V, 68.13V, 48.58V and 68.13V), case-III (51.64V, 67.39V, 51.64V and 67.39V) and case-IV (49.86V, 68.04V, 68.52V and 68.81) respectively.

TABLE 4. Power at GMPP of PV array configurations under shading cases.

Shading cases	Simulation				Experimental			
	SP	BL	HC	A-CT	SP	BL	HC	A-CT
Case-I	5.982	5.982	5.982	5.982	5.96	5.97	5.96	5.98
Case-II	5.392	5.392	5.392	5.392	5.435	5.383	5.40	5.365
Case-III	5.982	5.982	5.982	5.982	5.97	5.965	5.965	5.96
Case-IV	5.98	5.96	5.98	5.98	5.96	5.96	5.89	5.96

TABLE 5. Voltage at GMPP of PV array configurations under shading cases.

Shading cases	Simulation				Experimental			
	SP	BL	HC	A-CT	SP	BL	HC	A-CT
Case-I	65.5	65.73	65.5	65.9	65.18	66.24	66.66	65.73
Case-II	50.26	68.13	48.58	68.13	69.15	69.45	69.05	67.66
Case-III	51.64	67.39	51.64	67.39	52.98	51.39	51.92	66.87
Case-IV	49.86	68.04	68.52	68.81	49.86	68.42	68.42	68.84

TABLE 6. Power losses of PV array configurations under shading cases.

Shading cases	Simulation				Experimental			
	SP	BL	HC	A-CT	SP	BL	HC	A-CT
Case-I	63.5	58.2	62.8	55.6	65.9	58.7	62.9	58.2
Case-II	115.8	112.5	113.9	108.7	119.2	113.7	114.3	112.6
Case-III	128.6	127.1	122.2	112.2	130.4	129	126	114.9
Case-IV	156.5	148.7	154.6	144.76	157.5	149.4	154.1	147.4

TABLE 7. FF of PV array configurations under shading cases.

Shading cases	Simulation				Experimental			
	SP	BL	HC	A-CT	SP	BL	HC	A-CT
Case-I	0.57	0.581	0.57	0.586	0.569	0.566	0.575	0.581
Case-II	0.523	0.525	0.521	0.535	0.513	0.523	0.520	0.526
Case-III	0.442	0.446	0.4536	0.4744	0.4395	0.4456	0.4491	0.4689
Case-IV	0.390	0.404	0.389	0.410	0.396	0.404	0.399	0.409

(a) Power at GMPP for MATLAB/Simulink study

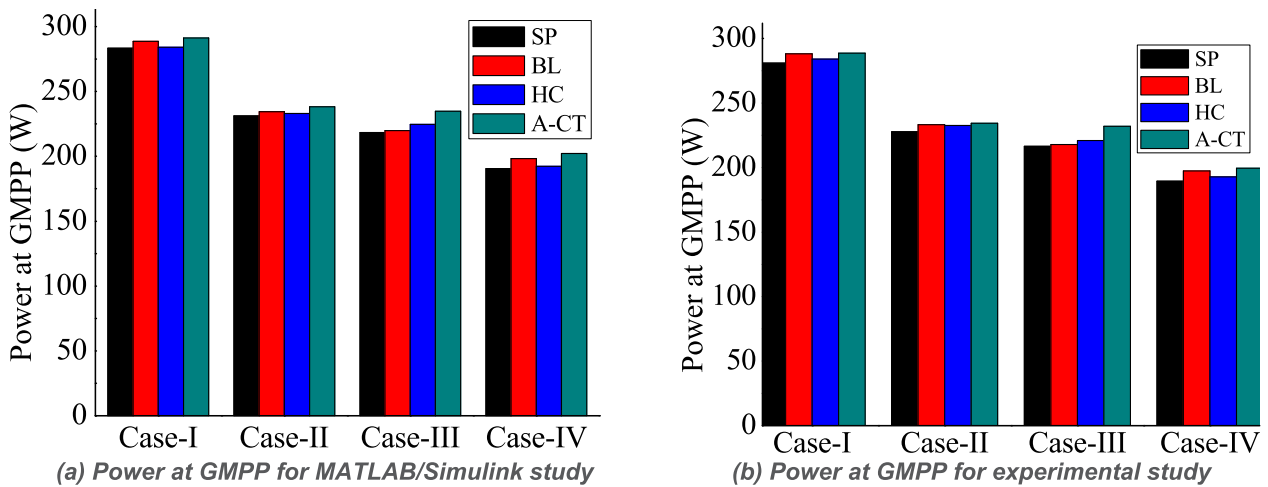(b) Power at GMPP for experimental study

FIGURE 12. (a)-(b) Power at GMPP.

During experimental study, voltage at GMPP for SP, BL, HC and A-CT configurations have distinguishing values under shading case-I (65.18V, 66.24V, 66.66V and 65.73V), case-II (69.15V, 69.45V, 69.05V and 67.66V) and case-III (52.98V, 51.39V, 51.92V and 66.87V), and case-IV (49.86V, 68.42V, 68.42V and 68.84) respectively. For a detailed quantitative analysis, the bar chart representation of the voltage at GMPP is shown in Fig. 12 and Table 5.

G. POWER LOSSES

The power losses due to the shading effect on PV systems such as SP, BL, HC and A-CT were recorded during
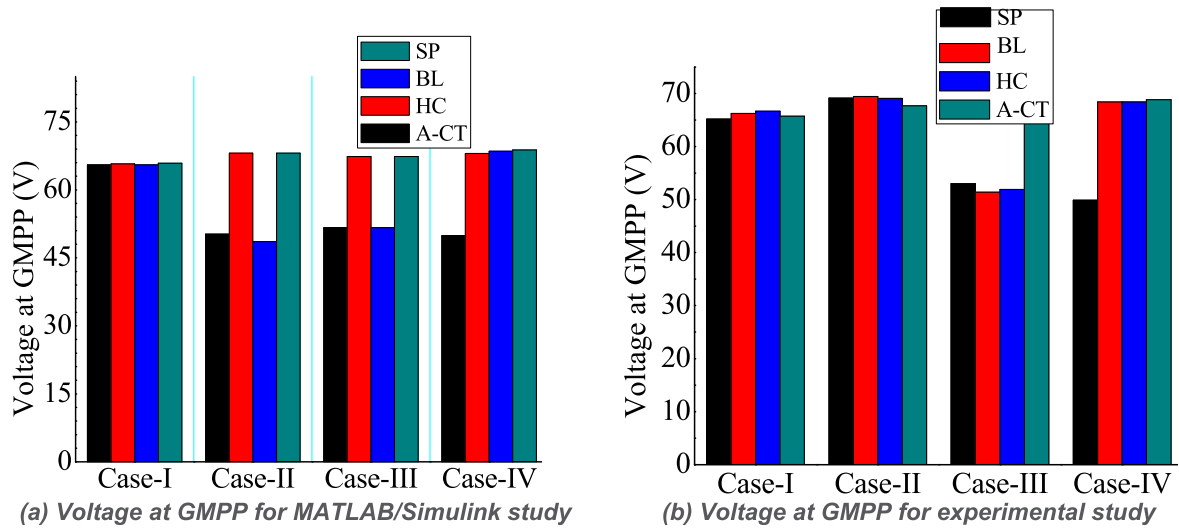
(a) Voltage at GMPP for MATLAB/Simulink study

(b) Voltage at GMPP for experimental study

FIGURE 13. (a)-(b) Power at GMPP.

(a) PL for MATLAB/Simulink study

(b) PL for experimental study

FIGURE 14. (a)-(b) Power losses.

(a) FF for MATLAB/Simulink study

(b) FF for experimental study

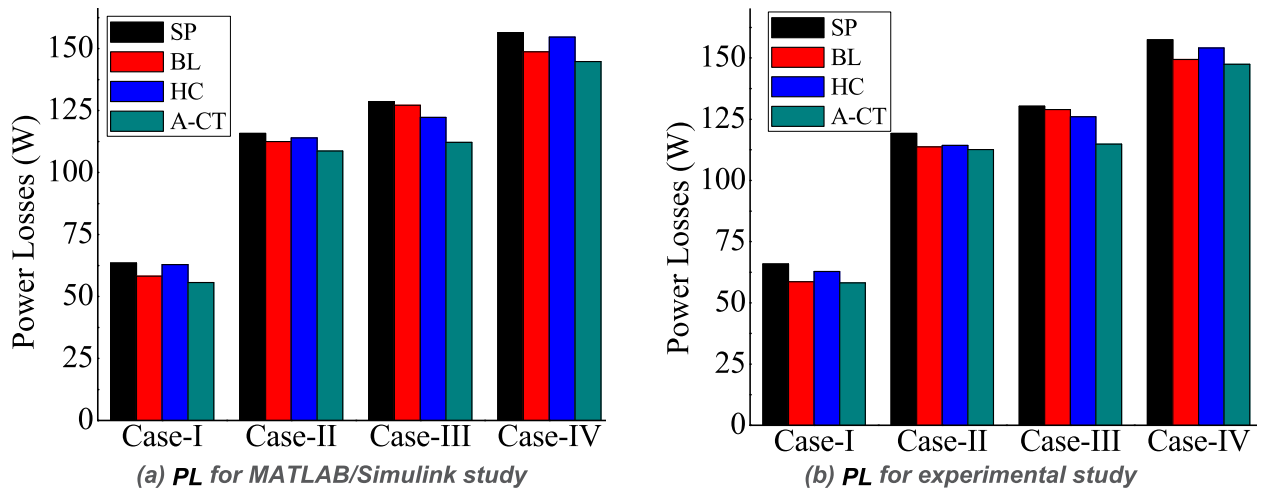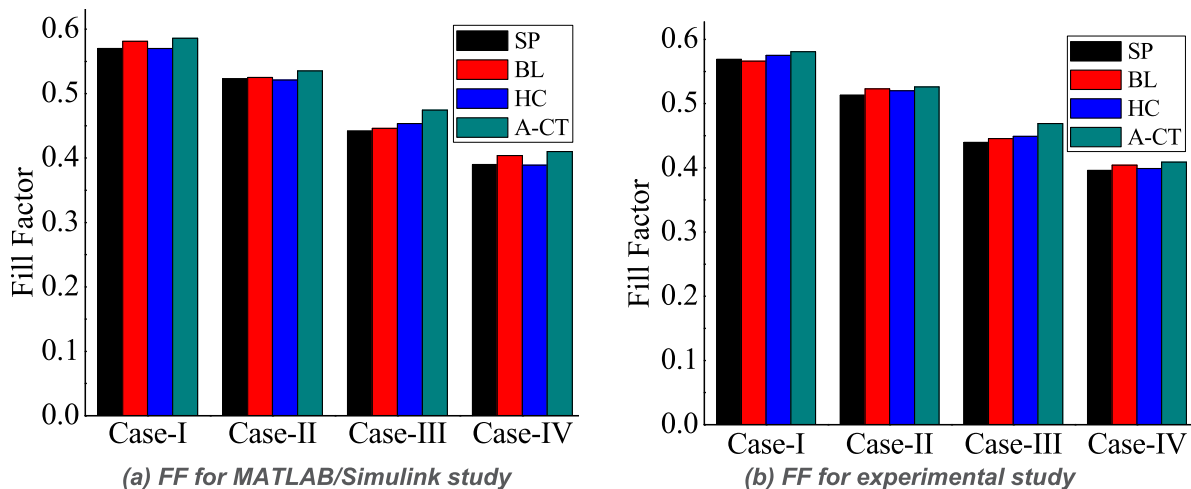**FIGURE 15.** (a)-(b) Fill factor assessment under PSCs.

MATLAB/Simulink study. Under shading cases I-IV, the A-CT configuration has minimum power losses of 55.6W, 108.7W, 112.2W and 144.76W. In addition, experimental

work is conducted and power losses are observed for all PV array configurations due to the shading effect. Minimum power losses such as 58.2W, 112.6W, 114.9W, and 147.4W

TABLE 8. PE (%) of PV array configurations under shading cases.

Shading cases	Simulation				Experimental			
	SP	BL	HC	A-CT	SP	BL	HC	A-CT
Case-I	--	1.83	0.875	2.71	--	2.49	1.05	2.66
Case-II	-	1.40	0.815	2.98	-	2.35	2.10	2.816
Case-III	-	0.68	2.84	6.98	-	0.642	1.99	6.59
Case-IV	-	3.9	0.98	5.80	-	4.10	1.35	5.06

TABLE 9. PR (%) of PV array configurations under shading cases.

Shading cases	Simulation				Experimental			
	SP	BL	HC	A-CT	SP	BL	HC	A-CT
Case-I	81.69	83.22	81.89	83.97	81.00	83.07	81.86	83.22
Case-II	66.81	67.56	67.16	68.66	65.63	67.22	67.05	67.54
Case-III	62.92	63.36	64.77	67.65	62.40	62.81	63.67	66.87
Case-IV	54.88	57.13	55.43	58.34	54.59	56.93	55.57	57.50

(a) PE for MATLAB/Simulink study   (b) PE for experimental study
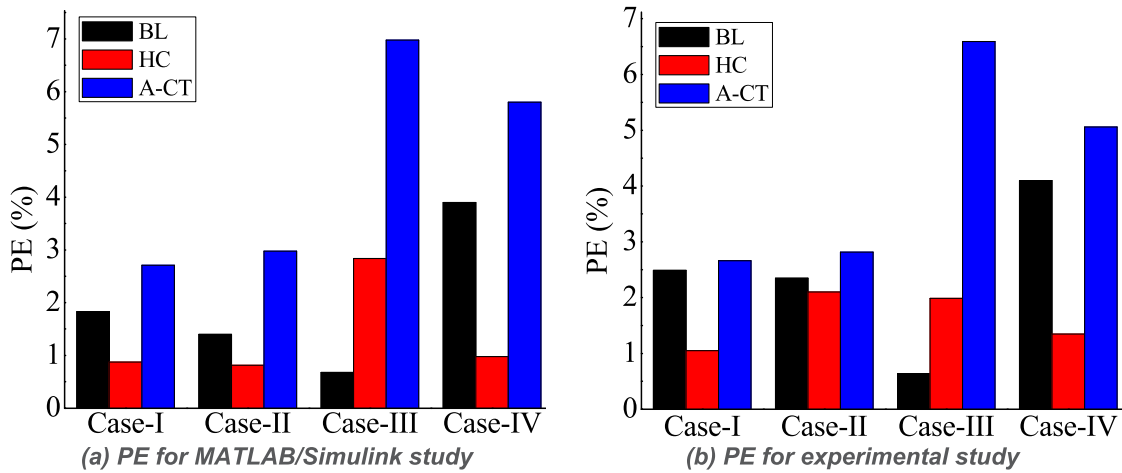
FIGURE 16. (a)-(b) PE assessment under PSCs.

(a) PR for MATLAB/Simulink study   (b) PR for experimental study
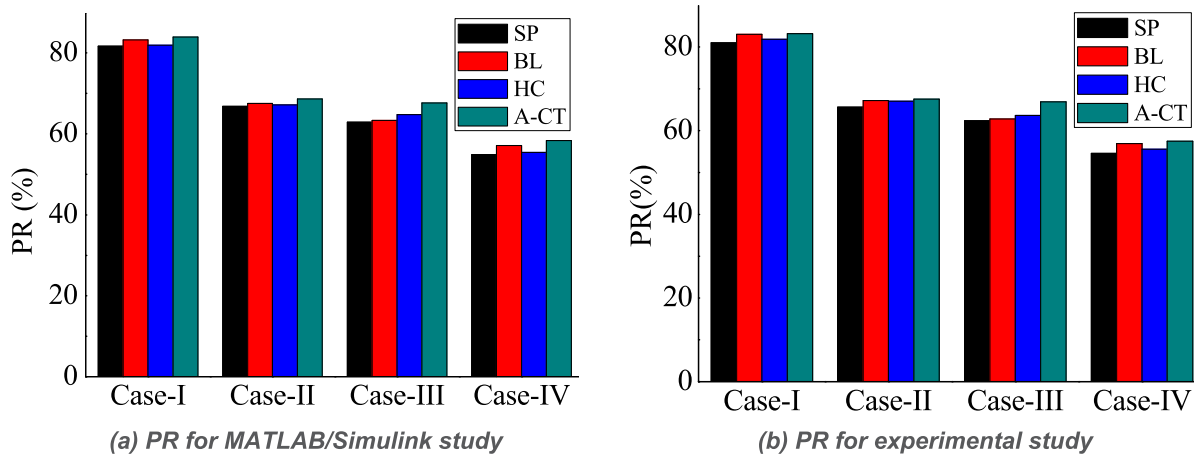
FIGURE 17. (a)-(b) PR assessment under PSCs.

were reported under shading scenarios for the A-CT configuration. In Table 6, quantitative analysis is shown along with the representation of the bar chart in Fig. 13.

H. FILL FACTOR
Dissimilarities in the FF due to the specific shading cases for the SP, BL, HC and A-CT arrangements compared to the bar chart in Figure 14. In shading cases I-IV in the MATLAB/Simulink analysis, A-CT improved FF by 0.586,.535, 0.474 and 0.410, respectively. The FF evaluation was conducted and it was found that A-CT had the highest values of 0.581, 0.526 and 0.468 and 0.409 for experimental studies in similar shading situations. The quantitative analysis of FF is depicted in Table 7.

I. POWER ENHANCEMENT

PE is the increment in power produced by the reconfigured PV array system due to shading dispersion and assessment is carried out with MATLAB/Simulink and experimental studies. During shading cases-I-IV, A-CT has highest PE with respect to SP configuration such as 2.71%, 2.98%, 6.98% and 5.80% respectively.

Furthermore, PE is observed as 2.66%, 2.816%, 6.59% and 5.06% during the experimental study. The PE for all the cases are shown in Table 8. Bar chart representation for PE is shown in figure 15 as,

J. PERFORMANCE RATIO

The performance of a PV array is determined by the performance ratio as indicated in Eq. (19). The quantitative analysis of PR is depicted in Table 9 and bar chart representation is shown in Fig. 16.

$$\%PR = \frac{P_m \ under \ shading \ conditions}{P_m \ at \ full \ irradiation} \qquad (19)$$

VI. CONCLUSION

This paper analysed and compared the performance of conventional SP, BL, HC configurations with new A-CT configuration under realistic shading cases: I-IV. The method used as a simplified reconfiguration technique can be extended to any size of the PV array, and performance key parameters such as power loss, PE, and FF were assessed with comprehensive comparative MATLAB/Simulink and experimental studies.

Thus, the proposed reconfiguration scheme for PV modules is particularly advantageous for the design of large PV plant. Novel A-CT configuration has lower number cross-tied connections between the parallel strings. Following key points of both the studies are as follows,

- For case-I: the performance parameters such as power at GMPP, FF, PE (w.r.t. SP) and minimized PL, and PR are found best as 291.3W, 0.586, 2.71%, 55.6W and 83.97% respectively for A-CT configuration through MATLAB/Simulation study under shading case-I. During experimental validation, similar performance parameters are observed and found as 288.7W, 0.581, 2.66%, 58.2W and 83.22%.
- Overall, A-CT has best values during MATLAB/Simulink and experimental studies under shading cases-II- IV for similar performance index.

The present study will be beneficial for commercial PV plants and new beginners in this area as a standard for future research work.

CONFLICT OF INTEREST

During the experimental study, there is no conflict of internet among all the authors.

REFERENCES

[1] J. W. Bishop, "Computer simulation of the effects of electrical mismatches in photovoltaic cell interconnection circuits," *Sol. Cells*, vol. 25, no. 1, pp. 73–89, Oct. 1988.

[2] A. Kovach and J. Schmid, "Determination of energy output losses due to shading of building-integrated photovoltaic arrays using a raytracing technique," *Sol. Energy*, vol. 57, no. 2, pp. 117–124, Aug. 1996.

[3] R. J. Mustafa, M. R. Gomaa, M. A. Dhaifallah, and H. Rezk, "Environmental impacts on the performance of solar photovoltaic systems," *Sustainability*, vol. 12, pp. 1–17, Jan. 2020.

[4] V. Quaschning and R. Hanitsch, "Numerical simulation of current-voltage characteristics of photovoltaic systems with shaded solar cells," *Sol. Energy*, vol. 56, no. 6, pp. 513–520, Jun. 1996.

[5] R. K. Pachauri, O. P. Mahela, A. Sharma, J. Bai, Y. K. Chauhan, B. Khan, and H. H. Alhelou, "Impact of partial shading on various PV array configurations and different modeling approaches: A comprehensive review," *IEEE Access*, vol. 8, pp. 181375–181403, 2020.

[6] H. Patel and V. Agarwal, "MATLAB-based modeling to study the effects of partial shading on PV array characteristics," *IEEE Trans. Energy Convers.*, vol. 23, no. 1, pp. 302–310, Mar. 2008.

[7] E. Karatepe, M. Boztepe, and M. Çolak, "Development of a suitable model for characterizing photovoltaic arrays with shaded solar cells," *Sol. Energy*, vol. 81, no. 8, pp. 977–992, Aug. 2007.

[8] L. Gao, R. A. Dougal, S. Liu, and A. P. Iotova, "Parallel-connected solar PV system to address partial and rapidly fluctuating shadow conditions," *IEEE Trans. Ind. Electron.*, vol. 56, no. 5, pp. 1548–1556, May 2009.

[9] D. Nguyen and B. Lehman, "An adaptive solar photovoltaic array using model-based reconfiguration algorithm," *IEEE Trans. Ind. Electron.*, vol. 55, no. 7, pp. 2644–2654, Jun. 2008.

[10] M. A. Chaaban, M. Alahmad, J. Neal, J. Shi, C. Berryman, Y. Cho, S. Lau, A. Schwer, Z. Shen, J. Stansbury, and T. Zhang, "Adaptive photovoltaic system," in *Proc. IEEE Conf. Ind. Electron. Saf.*, Nov. 2010, pp. 3192–3197.

[11] G. Velasco-Quesada, F. Guinjoan-Gispert, R. Pique-Lopez, M. Roman-Lumbreras, and A. Conesa-Roca, "Electrical PV array reconfiguration strategy for energy extraction improvement in grid-connected PV systems," *IEEE Trans. Ind. Electron.*, vol. 56, no. 11, pp. 4319–4331, Nov. 2009.

[12] D. Picault, B. Raison, S. Bacha, J. de la Casa, and J. Aguilera, "Forecasting photovoltaic array power production subject to mismatch losses," *Sol. Energy*, vol. 84, no. 7, pp. 1301–1309, Jul. 2010.

[13] F. Martínez-Moreno, J. Muñoz, and E. Lorenzo, "Experimental model to estimate shading losses on PV arrays," *Sol. Energy Mater. Sol. Cells*, vol. 94, no. 12, pp. 2298–2303, Dec. 2010.

[14] M. Z. S. El-Dein, M. Kazerani, and M. M. A. Salama, "Novel configurations for photovoltaic farms to reduce partial shading losses," in *Proc. IEEE Power Energy Soc. Gen. Meeting*, Jul. 2011, pp. 1–5.

[15] H.-L. Tsai, "Insolation-oriented model of photovoltaic module using MATLAB/Simulink," *Sol. Energy*, vol. 84, no. 7, pp. 1318–1326, Jul. 2010.

[16] S. Moballegh and J. Jiang, "Partial shading modeling of photovoltaic system with experimental validations," in *Proc. IEEE Conf. Power Energy Soc. Gen. Meeting*, Jul. 2011, pp. 1–9.

[17] P. dos Santos, E. M. Vicente, and E. R. Ribeiro, "Relationship between the shading position and the output power of a photovoltaic panel," in *Proc. 11th Brazilian Power Electron. Conf.*, Sep. 2011, pp. 676–681.

[18] H. Ziar, S. Mansourpour, E. Afjei, and M. Kazemi, "Bypass diode characteristic effect on the behavior of solar PV array at shadow condition," in *Proc. 3rd Power Electron. Drive Syst. Technol. (PEDSTC)*, Feb. 2012, pp. 1–5.

[19] K. Ding, X. Bian, H. Liu, and T. Peng, "A MATLAB-Simulink-based PV module model and its application under conditions of nonuniform irradiance," *IEEE Trans. Energy Convers.*, vol. 27, no. 4, pp. 864–872, Dec. 2012.

[20] M. Alahmad, M. A. Chaaban, S. K. Lau, J. Shi, and J. Neal, "An adaptive utility interactive photovoltaic system based on a flexible switch matrix to optimize performance in real-time," *Sol. Energy*, vol. 86, no. 3, pp. 951–963, Mar. 2012.

[21] T. S. Babu, D. Yousari, and K. B. Subramanian, "Photovoltaic array reconfiguration system for maximizing the harvested power using population-based algorithms," *IEEE Access*, vol. 6, pp. 1–16, 2016.

[22] A. Fathy, "Recent meta-heuristic grasshopper optimization algorithm for optimal reconfiguration of partially shaded PV array," *Sol. Energy*, vol. 171, pp. 638–651, Sep. 2018.

[23] R. Pachauri, A. S. Yadav, Y. K. Chauhan, A. Sharma, and V. Kumar, "Shade dispersion-based photovoltaic array configurations for performance enhancement under partial shading conditions," *Int. Trans. Electr. Energy Syst.*, vol. 28, no. 7, pp. 1–32, 2018.

[24] T. S. Babu, J. P. Ram, T. Dragicevic, M. Miyatake, F. Blaabjerg, and N. Rajasekar, "Particle swarm optimization based solar PV array reconfiguration of the maximum power extraction under partial shading conditions," *IEEE Trans. Sustain. Energy*, vol. 9, no. 1, pp. 74–85, Jan. 2018.

[25] G. Sai Krishna and T. Moger, "Improved SuDoKu reconfiguration technique for total-cross-tied PV array to enhance maximum power under partial shading conditions," *Renew. Sustain. Energy Rev.*, vol. 109, pp. 333–348, Jul. 2019.

[26] A. Ul-Haq, R. Alammari, A. Iqbal, M. Jalal, and S. Gul, "Computation of power extraction from photovoltaic arrays under various fault conditions," *IEEE Access*, vol. 8, pp. 47619–47639, 2020.

[27] G. Sagar, D. Pathak, P. Gaur, and V. Jain, "A Su Do Ku puzzle based shade dispersion for maximum power enhancement of partially shaded hybrid bridge-link-total-cross-tied PV array," *Sol. Energy*, vol. 204, pp. 161–180, Jul. 2020.

[28] D. Yousri, D. Allam, and M. B. Eteiba, "Optimal photovoltaic array reconfiguration for alleviating the partial shading influence based on a modified harris hawks optimizer," *Energy Convers. Manage.*, vol. 206, pp. 1–25, Feb. 2020.

[29] D. Yousri, T. S. Babu, S. Mirjalili, N. Rajasekar, and M. A. Elaziz, "A novel objective function with artificial ecosystem-based optimization for relieving the mismatching power loss of large-scale photovoltaic array," *Energy Convers. Manage.*, vol. 225, pp. 1–18, Dec. 2020.

[30] D. Yousri, S. B. Thanikanti, K. Balasubramanian, A. Osama, and A. Fathy, "Multi-objective grey wolf optimizer for optimal design of switching matrix for shaded PV array dynamic reconfiguration," *IEEE Access*, vol. 8, pp. 159931–159946, 2020.

[31] A. M. Ajmal, T. S. Babu, K. V. Ramachandaramurthy, D. Yousri, and J. B. Ekanayake, "Static and dynamic reconfiguration approaches for mitigation of partial shading influence in photovoltaic arrays," *Sustain. Energy Technol. Assessments*, vol. 40, pp. 1–23, Aug. 2020.

[32] R. Wang, Q. Sun, W. Hu, Y. Li, D. Ma, and P. Wang, "SoC-based droop coefficients stability region analysis of the battery for stand-alone supply systems with constant power loads," *IEEE Trans. Power Electron.*, vol. 36, no. 7, pp. 7866–7879, Jul. 2021.

[33] Q. Sun, R. Han, H. Zhang, J. Zhou, and J. M. Guerrero, "A multiagent-based consensus algorithm for distributed coordinated control of distributed generators in the energy Internet," *IEEE Trans. Smart Grid*, vol. 6, no. 6, pp. 3006–3019, Nov. 2015.

[34] X. Hu, H. Zhang, D. Ma, and R. Wang, "A tnGAN-based leak detection method for pipeline network considering incomplete sensor data," *IEEE Trans. Instrum. Meas.*, vol. 70, pp. 1–10, 2021.

[35] S. Vijayalekshmy, G. R. Bindu, and S. R. Iyer, "A novel Zig-Zag scheme for power enhancement of partially shaded solar arrays," *Sol. Energy*, vol. 135, pp. 92–102, Oct. 2016.

HASSAN HAES ALHELOU (Senior Member, IEEE) is currently a Faculty Member with Tishreen University, Latakia, Syria. He has published more than 100 research papers in the high quality peer-reviewed journals and international conferences. He has also performed reviews for high-prestigious journals, including IEEE Transactions on Industrial Informatics, IEEE Transactions on Industrial Electronics, *Energy Conversion and Management*, *Applied Energy*, and *International Journal of Electrical Power and Energy Systems*. He has participated in more than 15 industrial projects. His major research interests include power systems, power system dynamics, power system operation and control, dynamic state estimation, frequency control, smart grids, microgrids, demand response, load shedding, and power system protection. He is included in the 2018 and 2019 Publons list of the top 1% best reviewer and researchers in the field of engineering. He was a recipient of the Outstanding Reviewer Award from *Energy Conversion and Management* journal in 2016, *ISA Transactions* journal in 2018, *Applied Energy* journal in 2019, and many other Awards. He was a recipient of the Best Young Researcher in the Arab Student Forum Creative among 61 researchers from 16 countries at Alexandria University, Egypt, in 2011.

JIANBO BAI received the Ph.D. degree from Southeast University, in 2006. He was a Research Associate with The Hong Kong Polytechnic University, from 2007 to 2008. He acted as a Visiting Scholar with the Lawrence Berkeley National Laboratory, from 2013 to 2014. He has been serving as the Vice Dean of the College of Mechanical and Electrical Engineering, Hohai University, since 2016. His current research interests include comprehensive and highly efficient use of solar energy, and simulation and optimizing of PV power stations. He has hosted a project supported by the National Natural Science Foundation of China and two projects supported by the National Natural Science Foundation of Jiangsu Province in China. He has good research potential team and wide expertise area of research for such inspiration to our esteem participants.

RUPENDRA KUMAR PACHAURI received the B.Tech. degree from UP Technical University, Lucknow, India, in 2006, the M.Tech. degree from the Electrical Engineering Department, Faculty of Engineering and Technology, Zakir Husain College of Engineering and Technology, Aligarh Muslim University (AMU), Aligarh, India, in 2009, and the Ph.D. degree in renewable energy from G. B. University, India, in 2016. He is currently working as an Assistant Professor– Selection Grade with the Department of Electrical and Electronics Engineering, University of Petroleum and Energy Studies (UPES), Dehradun, India. He has published more than 75 research papers in International repute Science citation/Scopus indexed journals along with IEEE/Springer conferences. He has also performed reviews for high-prestigious journals, including IEEE Transactions on Industrial Informatics, IEEE Transactions on Industrial Electronics, *Renewable Energy*, *International Journal of Electrical Power and Energy Systems*, and *Solar Energy*. His research interests include solar energy, fuel cell technology, applications of ICT in PV systems, and smart grid operations.

MOHAMAD ESMAIL HAMEDANI GOLSHAN (Senior Member, IEEE) received the B.Sc. degree in electrical engineering from the Isfahan University of Technology, Isfahan, Iran, in 1987, the M.Sc. degree in electrical engineering from the Sharif University of Technology, Tehran, in 1990, and the Ph.D. degree in electrical engineering from the Isfahan University of Technology, in 1998. He is currently a Full Professor with the Department of Electrical and Computer Engineering, Isfahan University of Technology, where he is also a Professor. His major research interests include power system analysis, power system dynamics, power quality, dispersed generation, flexible ac transmission systems and custom power, and load modeling special arc furnace modeling.

• • •